Available online at www.sciencedirect.com
SCIENCE DIRECT
Earth and Planetary Science Letters 245 (2006) 260–277
EPSL
www.elsevier.com/locate/epsl

Strontium isotopes in melt inclusions from Samoan basalts: Implications for heterogeneity in the Samoan plume

Matthew G. Jackson [a,*], Stanley R. Hart [b]

[a] Massachusetts Institute of Technology–Woods Hole Oceanographic Institution Joint Program, Woods Hole, Massachusetts, 02543, USA
[b] Department of Geology and Geophysics, Woods Hole Oceanographic Institution, Woods Hole, Massachusetts, 02543, USA

Received 25 October 2005; received in revised form 22 February 2006; accepted 26 February 2006
Available online 19 April 2006
Editor: R.W. Carlson

Abstract

We measured $^{87}Sr/^{86}Sr$ ratios on 41 olivine-hosted melt inclusions from nine Samoan basalts using laser ablation multi-collector (LA-MC) ICPMS. $^{87}Sr/^{86}Sr$ ratios are corrected for mass bias after eliminating major isobaric interferences from Rb and Kr. The external precision averages ±320 ppm (2σ) for the $^{87}Sr/^{86}Sr$ ratios on natural Samoan basalt glass standards of a similar composition to the melt inclusions.

All of the Sr-isotope ratios measured by LA-MC-ICPMS on Samoan melt inclusions fall within the range measured on whole-rocks using conventional methods. However, melt inclusions from two Samoan basalt bulk rock samples are extremely heterogeneous in $^{87}Sr/^{86}Sr$ (0.70459–0.70926), covering 70% of the variability observed in ocean island basalts worldwide and nearly all of the variability observed in the Samoan island chain (0.7044–0.7089). Seven melt inclusions from a third high $^{3}He/^{4}He$ Samoan basalt are isotopically homogeneous and exhibit $^{87}Sr/^{86}Sr$ values from 0.70434 to 0.70469.

Several melt inclusions yield $^{87}Sr/^{86}Sr$ ratios higher than their host rock, indicating that assimilation of oceanic crust and lithosphere is not the likely mechanism contributing to the isotopic variability in these melt inclusions. Additionally, none of the 41 melt inclusions analyzed exhibit $^{87}Sr/^{86}Sr$ ratios lower than the least radiogenic basalts in Samoa ($^{87}Sr/^{86}Sr=0.7044$), within the quoted external precision. This provides an additional argument against assimilation of oceanic crust and lithosphere as the source of the isotopic diversity in the melt inclusions.

The trace element and isotopic diversity in Samoan melt inclusions can be modeled by aggregated fractional melting of two sources: A high $^{3}He/^{4}He$ source and an EM2 (enriched mantle 2) source. Melts of these two sources mix to generate the isotopic diversity in the Samoan melt inclusions. However, the melt inclusions from a basalt with the highest $^{3}He/^{4}He$ ratios in Samoa exhibit no evidence of an enriched component, but can be modeled as melts of a pure high $^{3}He/^{4}He$ mantle source.

Keywords: $^{87}Sr/^{86}Sr$; laser ablation; MC-ICPMS; melt inclusion; Samoa; EM2; PHEM; FOZO

1. Introduction

Ocean island basalts (OIBs) erupted at hotspots are thought to be the surface expression of buoyantly upwelling mantle plumes that sample the mantle's compositional heterogeneities at various depths and times

* Corresponding author. Tel.: +1 508 289 3490; fax: +1 508 457 2175.
E-mail address: mjackson@whoi.edu (M.G. Jackson).

0012-821X/$ - see front matter © 2006 Elsevier B.V. All rights reserved.
doi:10.1016/j.epsl.2006.02.040

[1,2]. The Samoan islands and seamounts, formed by a mantle plume impinging on the Pacific plate just north of the Tonga Trench, form a time-progressive hotspot track [3,4] which conforms reasonably well to Morgan's hotspot model [5]. Samoan lavas exhibit the highest $^{87}Sr/^{86}Sr$ ratios and the largest $^{87}Sr/^{86}Sr$ variation (0.7044–0.7089) measured in fresh OIBs [4,6], making them ideal for prospecting for diverse Sr-isotope compositions in melt inclusions.

Olivine-hosted melt inclusions in Samoan lavas provide snapshots of diverse magma chemistry before complete melt aggregation, providing an opportunity to see more of the isotopic heterogeneity which exists in the melt source but that is not detectable in whole rocks. However, the chemical variability in melt inclusions may be generated by a number of processes that obscure source variation, including pre-entrapment fractional crystallization, post-entrapment diffusive re-equilibration, crustal assimilation, and degree, type and depth of melting [7–16].

Studies delineating Pb-isotope diversity in melt inclusions have demonstrated that heterogeneous melt source compositions are an important factor in generating compositional variability [17–21]. A landmark Pb-isotope study of melt inclusions hosted in basalts from Mangaia Island in the Cook Islands revealed significantly more isotopic heterogeneity than is found in whole rocks from the island [17]. The results indicate the presence of an unradiogenic Pb-isotope endmember in the melt inclusions not discernable in whole-rock basalts. Problematically, this unradiogenic Pb endmember has been poorly characterized, owing partly to the large uncertainties associated with in situ Pb-isotope measurements: Pb-isotope data from melt inclusions generally are limited to $^{208}Pb/^{206}Pb$ versus $^{207}Pb/^{206}Pb$ isotope projections (due to the inability to collect precise ^{204}Pb data on silicate melt inclusions), which place DMM (depleted MORB mantle, low $^{3}He/^{4}He$, low $^{87}Sr/^{86}Sr$), FOZO (*Fo*cus *Zo*ne, high $^{3}He/^{4}He$, low $^{87}Sr/^{86}Sr$), PHEM (*P*rimitive *He*lium *M*antle, high $^{3}He/^{4}He$, middle-range $^{87}Sr/^{86}Sr$) and EM2 (enriched mantle 2, low $^{3}He/^{4}He$, high $^{87}Sr/^{86}Sr$) in such close graphical proximity that they cannot be unequivocally resolved. The true pedigree of the unradiogenic Pb endmember in Mangaia is still unknown, and could be similar to any of these four endmembers.

An advantage to the Sr-isotope system is that the EM2 endmember has dramatically higher $^{87}Sr/^{86}Sr$ ratios (~0.7089) [4] than the DMM (0.7026) [22], PHEM (0.7045) [23] and FOZO (0.7030) [24] mantle endmembers, and can be readily differentiated from the three less radiogenic endmembers. PHEM hosts significantly more radiogenic Sr than DMM and FOZO and is easily resolved from these two components. Unfortunately, DMM and FOZO exhibit similar $^{87}Sr/^{86}Sr$ ratios and it will be difficult to differentiate between these two components as potential sources of the isotopic diversity in melt inclusions.

We present Sr-isotope data from olivine-hosted melt inclusions recovered from Samoan basalts, some of which lie near the EM2 mantle endmember, with the goal of better understanding the puzzling unradiogenic component sampled by melt inclusions. To this end, we also contribute Sr-isotope data measured on melt inclusions from a recently discovered high $^{3}He/^{4}He$ basalt from Samoa [25]. Our strategy is to analyze Sr isotopes in melt inclusions from EM2 and high $^{3}He/^{4}He$ endmember basalts from Samoa, to constrain the role of the various components–EM2, PHEM, DMM and FOZO–that may be contributing to the Sr-isotope diversity in the Samoan plume.

2. Methods

A detailed description of the protocol used for in situ measurement of Sr isotopes in basaltic glasses (and melt inclusions) by LA-MC-ICPMS is provided in the Supplementary data. In order to measure Sr-isotope ratios in situ, we use a 213 nm NewWave laser ablation system coupled to a Themo-Finnigan Neptune MC-ICPMS, located in the Plasma Facility at Woods Hole Oceanographic Institution (WHOI). During analytical runs, the laser is run in aperture mode with 100% power, a pulse rate of 20 Hz and a spot size of 120 μm. The raster pattern varies depending on the size and shape of the melt inclusion, and the line speed is 4 μm/s. Surface contamination is removed by pre-ablation using the same raster and spot size, but with a pulse rate of 5 Hz, 45% power and a raster speed of 30 μm/s.

During each analytical session, we measure intensities on masses 82 through 88. Raw data are exported to an offline data correction program (TweaKr) for correcting the Rb and Kr isobaric interferences. Runs with low intensities (i.e., <1 V on mass 88, due to small size or low Sr content) were discarded as they are prone to large systematic errors [26]. Masses 85 and 88 are pure Rb and Sr, respectively, with no significant known interferences, and require correction only for mass fractionation. We correct for Kr interferences on masses 84 and 86 so that the mass fractionation-corrected $^{84}Sr/^{86}Sr$ value is canonical (0.0565725). The protocol for correcting mass 87 for the Rb interference is the following: A Samoan basalt glass with known $^{87}Sr/^{86}Sr$, from analysis by conventional Thermal Ionization Mass Spectrometry

Table 1
Corrected and normalized $^{87}Sr/^{86}Sr$ melt inclusion and whole-rock data, including Rb/Sr ratios and raw exported Neptune data (in volts)

Sample name and grain #	Disc #	Mass 82 meas'd-V	Mass 83 meas'd-V	Mass 84 meas'd-V	Mass 85 meas'd-V	Mass 86 meas'd-V	Mass 87 meas'd-V	Mass 88 meas'd-V	$^{85}Rb/^{87}Rb$ required	$^{87}Sr/^{86}Sr$ corr'd [a]	$^{87}Sr/^{86}Sr$ corr'd [b]	Int. prec.	Rb/Sr	Int. prec.	# Cycles	Type	Oliv Fo
AVON3-78-1 (whole rock):											0.70890		0.1255				
78-1Z	Year1	0.0013	0.0011	0.0193693	0.158083	0.263023	0.250903	2.25759	2.58966	0.70791	0.70784	87	0.0746	1.82	14[c]	C	84.6
78-1#7[d]	Disc1	0.0020	0.0022	0.0193323	0.164332	0.188415	0.199670	1.60867	2.58811	0.70927	0.70926	123	0.1081	2.47	9	H	84.6
78-1#9[d]	Disc1	0.0019	0.0021	0.0178511	0.111482	0.163039	0.159876	1.38845	2.58811	0.70733	0.70732	103	0.0850	1.90	6	H	84.4
78-1#6[d]	Disc2	0.0031	0.0034	0.0297219	0.341900	0.308400	0.354647	2.62064	2.58593	0.70846	0.70843	99	0.1397	2.63	32	H	83.6
78-1#9[d]	Disc2	0.0031	0.0034	0.0316443	0.384820	0.340724	0.395010	2.89882	2.58593	0.70873	0.70870	94	0.1421	3.08	30	H	82.8
78-1#10[d]	Disc2	0.0030	0.0031	0.0241696	0.094343	0.202069	0.179689	1.70410	2.58663	0.70845	0.70842	104	0.0593	3.21	16	H	83.6
78-1#4[d]	Disc3	0.0049	0.0057	0.0638080	0.704962	0.756968	0.817352	6.43584	2.58694	0.70869	0.70866	44	0.1179	0.60	40	G	85.2
78-1inside	Disc3	0.0048	0.0049	0.0311385	0.155536	0.152840	0.165959	1.25071	2.58564	0.70689	0.70686	139	0.1337	2.20	16	C	84.3
78-1B	Disc3	0.0044	0.0043	0.0327454	0.189114	0.222802	0.230356	1.86119	2.58675	0.70791	0.70788	127	0.1089	5.76	10	C	84.2
78-1C	Disc3	0.0041	0.0043	0.0408646	0.414636	0.401444	0.448986	3.40453	2.58675	0.70866	0.70863	38	0.1304	1.96	24	C	83.9
78-1D	Disc3	0.0048	0.0048	0.0313504	0.130366	0.156852	0.158811	1.28485	2.58675	0.70699	0.70696	119	0.1091	3.79	14	C	85.3
AVON3-71-2 (whole rock):											0.70594		0.0754				
71-2C[d]	Year1	0.0015	0.0012	0.0241555	0.131881	0.348997	0.301171	2.99950	2.58977	0.70488	0.70481	50	0.0469	4.99	10[c]	G	88.8
71-2C[e]	Disc3	0.0049	0.0051	0.0423813	0.151006	0.357484	0.309961	3.00928	2.58772	0.70487	0.70484	60	0.0539	2.09	19	G	88.8
71-2Da	Year1	0.0014	0.0012	0.0190549	0.143364	0.258958	0.241512	2.22256	2.58977	0.70555	0.70549	53	0.0687	3.92	12[c]	C	90.1
71-2i_mi1[d]	Disc1	0.0041	0.0042	0.0293387	0.151118	0.188888	0.190950	1.57393	2.58696	0.70605	0.70602	42	0.1028	0.89	19	G	90.7
71-2#6_saol1	Disc1	0.0040	0.0044	0.0392836	0.237282	0.399731	0.376067	3.39132	2.58675	0.70532	0.70529	63	0.0750	2.45	32	C	90.3
71-2#6_saol2	Disc1	0.0038	0.0039	0.0311684	0.151330	0.259691	0.241924	2.18859	2.58675	0.70511	0.70508	90	0.0741	3.15	15	C	90.5
71-2pentagon	Disc1	0.0035	0.0036	0.0274768	0.164455	0.221630	0.220515	1.86556	2.58653	0.70603	0.70600	69	0.0944	1.40	35	C	91.1
71-2#5[d]	Disc3	0.0049	0.0055	0.0608667	0.440578	0.704362	0.672560	5.98503	2.58694	0.70537	0.70534	34	0.0792	1.23	40	G	91.0
71-2#5[e]	Disc3	0.0049	0.0057	0.0600272	0.456791	0.688053	0.667289	5.84446	2.58694	0.70537	0.70534	34	0.0841	1.21	40	G	91.0
71-2#6[d]	Disc3	0.0050	0.0053	0.0461581	0.261970	0.420138	0.399032	3.54513	2.58674	0.70602	0.70600	53	0.0794	1.35	40	G	85.7
71-2#6[e]	Disc3	0.0050	0.0054	0.0511361	0.320998	0.514222	0.489758	4.35389	2.58674	0.70600	0.70598	32	0.0793	1.19	40	G	85.7
71-2Z	Disc3	0.0041	0.0042	0.0286629	0.120538	0.176062	0.169532	1.46336	2.58809	0.70576	0.70573	97	0.0882	2.60	21	C	86.1
71-2N	Disc3	0.0041	0.0043	0.0326106	0.171904	0.249420	0.242412	2.09517	2.58778	0.70554	0.70551	48	0.0879	2.74	26	C	90.5
71-2imi_run2	Disc3	0.0046	0.0048	0.0392641	0.162916	0.326152	0.292704	2.74335	2.58778	0.70520	0.70518	112	0.0638	2.80	12	C	91.0
71-2V	Disc3	0.0034	0.0037	0.0358138	0.196791	0.370738	0.339729	3.15166	2.58754	0.70461	0.70459	122	0.0668	4.32	13	C	87.4
OFU-04-06 (whole rock):											0.70458		0.0458				
OFU-04-06-13[d]	Ofu	0.0012	0.0004	0.0123598	0.087599	0.202878	0.179279	1.74009	2.58774	0.70458	0.70457	226	0.0541	6.04	6	H	79.8
OFU-04-06-15[d]	Ofu	0.0008	0.0006	0.0166800	0.116272	0.260130	0.231639	2.23575	2.58791	0.70443	0.70443	128	0.0556	1.62	13	H	77.3

OFU-04-06-25[d]	Ofu	0.0009	0.0008	0.0272537	0.215485	0.450579	0.407078	3.87445	2.58797	0.70455	0.70454	60	0.0595	3.24	20	H	77.2
OFU-04-06-26[d]	Ofu	0.0007	0.0006	0.0135577	0.076760	0.200599	0.173323	1.72195	2.58771	0.70443	0.70443	86	0.0476	2.73	16	H	76.5
OFU-04-06-28[d]	Ofu	0.0007	0.0006	0.0138764	0.082936	0.207139	0.180426	1.77796	2.58777	0.70435	0.70434	164	0.0499	1.97	11	H	78.4
OFU-04-06-03[d]	Ofu	0.0004	0.0005	0.0090473	0.057761	0.131245	0.115793	1.11700	2.58747	0.70443	0.70443	92	0.0560	2.67	15	H	83.8
OFU-04-06-02[d]	Ofu	0.0007	0.0006	0.0126725	0.082453	0.187441	0.166696	1.61548	2.58588	0.70469	0.70469	184	0.0542	0.96	7	H	76.5
AVON3-71-11 (whole rock):											0.70550		0.0700				
71-11a[d]	Disc1	0.0035	0.0035	0.0250240	0.083017	0.152405	0.138888	1.27387	2.58654	0.70653	0.70653	83	0.0691	1.22	16	G	83.0
71-11a[e]	Disc1	0.0019	0.0021	0.0204900	0.125897	0.216562	0.204083	1.85257	2.58857	0.70692	0.70692	109	0.0720	0.92	15	G	83.0
71-11#1[d]	Disc3	0.0048	0.0048	0.0316250	0.103649	0.160366	0.150752	1.31592	2.58772	0.70683	0.70680	144	0.0846	5.70	8	G	81.4
AVON3-68-3 (whole rock):											0.70539		0.0688				
68-3#6mi1[d]	Disc1	0.0020	0.0021	0.0186133	0.117638	0.165627	0.163878	1.40909	2.58798	0.70625	0.70624	75	0.0884	3.01	20	G	87.9
68-3#6mi2	Disc1	0.0038	0.0040	0.0305189	0.209211	0.258789	0.264567	2.18215	2.58653	0.70577	0.70575	87	0.1027	1.92	12	C	87.9
68-3#6mi2[e]	Disc1	0.0037	0.0041	0.0371899	0.294848	0.389761	0.392493	3.31142	2.58653	0.70577	0.70574	93	0.0954	1.73	9	C	87.9
68-3Ami	Disc3	0.0041	0.0042	0.0302365	0.092078	0.197293	0.173102	1.64414	2.58754	0.70482	0.70480	144	0.0600	6.45	10	C	90.1
AVON3-63-2 (whole rock):											0.70540		0.0679				
63-2mi	Disc3	0.0049	0.0051	0.0641890	0.514757	0.759082	0.741869	6.46111	2.58815	0.70599	0.70596	58	0.0856	2.68	31	C	–
63-2mi[e]	Disc3	0.0047	0.0056	0.0601701	0.544474	0.708353	0.718034	6.03171	2.58815	0.70616	0.70613	69	0.0969	1.22	36	C	–
63-2ami	Disc3	0.0044	0.0045	0.0283814	0.086324	0.138106	0.128251	1.13104	2.58815	0.70522	0.70520	181	0.0818	4.84	11	C	87.1
63-2bmi1	Disc3	0.0044	0.0045	0.0334163	0.133112	0.234231	0.215648	1.95929	2.58815	0.70528	0.70525	55	0.0728	3.15	23	C	86.6
AVON3-74-1 (whole rock):											0.70469		0.0484				
74-1mi	Year1	0.0015	0.0012	0.0174643	0.076749	0.224099	0.189719	1.91969	2.58895	0.70483	0.70477	157	0.0426	1.38	9[c]	C	85.1
S11 (whole rock):											0.70620		0.0597				
S11mi	Disc3	0.0048	0.0048	0.0330920	0.078499	0.189324	0.161268	1.56507	2.58564	0.70520	0.70518	125	0.0539	6.13	11	C	76.5
AVON3-78-3 (whole rock):											0.70889		0.1108				
78-3 mi	Year1	0.0014	0.0012	0.0184433	0.207247	0.241204	0.254752	2.06790	2.58966	0.70814	0.70807	61	0.1068	3.51	18[c]	C	84.1

All samples, except for OFU-04-06 and S11, are dredge samples from the AVON3 dredging cruise. Melt inclusion type refers to whether it was homogenized (H), glassy (G) or crystalline (C). Host olivine forsterite contents are given in the last column. Internal precision (Int. prec.) is standard error (2σ) and is in ppm ($^{87}Sr/^{86}Sr$) or % (Rb/Sr). Melt inclusion $^{87}Sr/^{86}Sr$ ratios are corrected for the isobaric interference from Rb by use of the bracketing method (see text for details). All melt inclusion analyses were performed on 01/27/04, 01/10/05, 01/11/05, 08/09/05 and 08/10/06 and corrected for the isobaric Rb interference using the Samoan glass standard analyses from those 5 days (see Supplementary data). Melt inclusion Sr-isotope and Rb/Sr data from a particular sample are listed immediately below the equivalent whole-rock data.

[a] Sr-isotopes are corrected for Kr and Rb interferences and fractionation-corrected.

[b] After correction for Rb and Sr interferences and fractionation, melt inclusions are corrected for 987 standard solution runs for each analytical session.

[c] Cycle length for melt inclusions from disc "Year1" are 16 s integrations during analysis. Cycles for all other measurements are 8 s integration.

[d] Has major and/or trace element data in Table 2.

[e] Replicate analysis of a melt inclusion is listed immediately below first analysis. Six melt inclusions were large enough to permit replicate analyses. Melt inclusion sample Year1_71-2 was replicated over a 1-year period, and was renamed Disc3_71-2C for the replicate analysis. All other replicate analyses were made during the same analytical session.

(TIMS), is measured by laser ablation, Kr-corrected, and the $^{85}Rb/^{87}Rb$ ratio is adjusted until the known TIMS $^{87}Sr/^{86}Sr$ value of the glass is achieved. We adopted the strategy of using the required $^{85}Rb/^{87}Rb$ of the Samoan basalt glass standards to bracket the $^{85}Rb/^{87}Rb$ of the basalt glass unknowns. In order to estimate the overall accuracy associated with this technique, we apply contiguous bracketing of the glass standard runs, and we are able to reproduce the known TIMS values to within an average of ±320 ppm (2σ standard deviation). However, due to uncertainty associated with the $^{85}Rb/^{87}Rb$ ratio (2.5875±0.00275, 2σ), the final, corrected $^{87}Sr/^{86}Sr$ ratio exhibits an error magnification that is directly proportional to the Rb/Sr ratio of the sample. Samples with low Rb/Sr will exhibit less error from the Rb correction (145 ppm, Rb/Sr=0.04) than samples with high Rb/Sr (505 ppm, Rb/Sr=0.14) (see Supplementary data). However, over the range of Rb/Sr in the Samoan basalt glass standards (0.045-0.126), we find no relationship between the internal (in-run) precision of $^{87}Sr/^{86}Sr$ ratios (which average 45 ppm, 2ó standard deviation) and Rb/Sr during analyses of basalt glasses by laser ablation. Similarly, there does not appear to be a relationship between Kr/Sr and the internal precision or reproducibility (external precision) of the $^{87}Sr/^{86}Sr$ ratios in Samoan glass standards over the range of ratios that we have observed during melt inclusion analysis ($^{82}Kr/^{88}Sr$ from 0.00013 to 0.004). Finally, the reproducibility of $^{87}Sr/^{86}Sr$ measurement does not appear to be related to Sr intensity over the range of Sr intensities observed in lasering Samoan glasses, a range that encompasses the melt inclusion analyses.

Six melt inclusions were large enough for replicate analysis (one melt inclusion, 71-2C, was replicated over a one-year period), and five of their $^{87}Sr/^{86}Sr$ ratios were reproducible within the quoted precision. However, the replicate analysis of melt inclusion 71-11a was different by 550 ppm (see Table 1), while error resulting from the Rb correction is only 260 ppm (2σ) on Samoan glass standards with similar Rb/Sr ratios. The internal precision of the replicate analysis of this melt inclusion was ~100 ppm (2σ). Data from this melt inclusion indicates that larger-than-usual $^{85}Rb/^{87}Rb$ variations over time can occasionally generate uncertainties (above the 2σ level) in $^{87}Sr/^{86}Sr$ that are somewhat larger than error predicted by the data from Samoan glass standards.

An upper limit for the $^{87}Sr/^{86}Sr$ measurement precision on Samoan melt inclusions with low Rb/Sr can be inferred from the near-uniform ratios obtained on melt inclusions from the high $^{3}He/^{4}He$ Ofu basalt. The Rb/Sr values were among the lowest during analysis of Ofu melt inclusions, and the tight clustering of the Ofu melt inclusions may be partially explained by decreased error of $^{87}Sr/^{86}Sr$ measurement for these samples compared to other, higher Rb/Sr Samoan glasses and melt inclusions from Vailulu'u and Malumalu. If we assume that the Ofu melt inclusions are isotopically homogeneous, then the external precision on these 7 melt inclusions is ±335 ppm (2σ). Some of the apparent variability may be a result of error from the Rb correction, which is ±190 ppm (2σ) at Rb/Sr ratios of 0.053, and may not reflect true variability. Additionally, internal precision varied from 60 to 226 ppm (2σ standard error) on the seven Ofu melt inclusions.

Masses 85 and 88 represent pure Rb and Sr, respectively, so that fairly precise measurement of Rb/Sr ratios can be generated. After correcting for mass fractionation (≈1.5%/amu), Rb/Sr ratios on Samoan basalt glasses measured by laser ablation are reproduceable to 17% (2σ, compared to ratios obtained by XRF/ICP techniques on the same samples), and precise (1.7%, 2σ) during multiple runs on the same glass (see Supplementary data).

Major element compositions of glassy and homogenized melt inclusions were obtained with a JEOL-733 automated electron microprobe at the Massachusetts Institute of Technology using an electron beam with current of 10 nA and accelerating potential of 15 kV focused to a spot of 1–2 μm in diameter for olivine analyses, and defocused to 10 μm for glass analyses. Trace element contents were determined with a Cameca IMS 3f ion microprobe following the techniques described in [27,28]. A small beam (5 μm diameter spot), combined with a high-energy filtering technique (80–100 eV window), was used to determine trace element concentrations. Precision for Sr, La, Zr, Y is estimated to be ±15%, and ±20–30% for Ba, Nb and Rb. Homogenization of olivine-hosted melt inclusions was performed in a furnace at 1187–1220 C (depending on olivine composition) at 1 atm pressure for 5 min in a graphite capsule.

To correct for the effects of crystallization of olivine in the glassy and homogenized melt inclusions, we add equilibrium olivine to the melt inclusions in 0.1% increments until equilibrium with mantle olivine (Fo_{90}) is achieved, assuming olivine-melt partitioning of Fe and Mg from [29]. Instead of correcting the melt inclusions to be in equilibrium with the host olivine, this correction scheme is chosen so that we can compare them to similarly corrected Samoan whole-rock lavas (after discarding data from the most evolved–MgO<6.5 wt.%–whole-rock samples).

3. Results

3.1. Sr-isotope variability in melt inclusions

Sr-isotopes were measured in melt inclusions from nine geochemically well-characterized basalt samples [4,25] from five islands and seamounts located along the Samoan hotspot track. Olivines ($Fo_{76–91}$) with large ellipsoidal melt inclusions (50–250 μm diameter) were separated from the basalt samples for melt inclusion exposure and isotopic analysis. Most of the melt inclusions were crystalline and usually contained dendritic clinopyroxene in a glassy matrix, with spinel and rare sulfide globules; some (≈5%) of the melt inclusions were glassy. The high $^3He/^4He$ basalt sample OFU-04-06 was unique in that amphibole and apatite were common melt inclusion phases, and carbonate was also observed.

Olivines ($Fo_{82–85}$) hosting melt inclusions were separated from Malumalu seamount dredge sample 78-1, a picrite with the highest $^{87}Sr/^{86}Sr$ ratio (0.7089) of any OIB [4]. Melt inclusion-rich olivines were also recovered from dredge sample 71-2 ($Fo_{84–91}$) from Vailulu'u, a seamount that displays intermediate enrichment relative to the other Samoan islands and seamounts (bulk rock $^{87}Sr/^{86}Sr$ isotope ratios from 0.7052 to 0.7067, $n=20$). From Ofu Island, olivines ($Fo_{76–84}$) were recovered from ankaramite dike sample OFU-04-06, which exhibits the highest $^3He/^4He$ measured in a Samoan basalt [25]. Lavas from Ofu are the most isotopically homogeneous of the volcanoes in the Samoan chain ($^{87}Sr/^{86}Sr$ from 0.70444 to 0.70480, $n=12$). Finally, a smaller number of olivines were separated for melt inclusion analysis from Vailulu'u dredge samples 71-11 ($Fo_{81–83}$), 63-2 ($Fo_{86–87}$) and 68-3 ($Fo_{87–90}$), Malumalu dredge sample 78-3 (Fo_{84}), Ta'u Island dredge sample 74-1 (Fo_{85}), and Savai'i subaerial post-erosional sample S11 (Fo_{76}).

The Sr-isotope data from melt inclusions in just three Samoan whole-rock samples (OFU-04-06, 78-1 and 71-2) define a broad array that encompasses the entire spectrum of Sr-isotope variability (0.70434–0.70926) recorded in Samoan basalts (Fig. 1 and Table 1). Eleven melt inclusions from 78-1 display $^{87}Sr/^{86}Sr$ values of 0.70686–0.70926, and encompass over 30% of the isotope variability observed in the OIB mantle. Vailulu'u melt inclusions from dredge samples 71-2 ($^{87}Sr/^{86}Sr=0.70459–0.70602$, $n=12$ melt inclusions) and 68-3 ($^{87}Sr/^{86}Sr=0.70480–0.70624$, $n=3$) exhibit a smaller range of Sr-isotope values than 78-1. However, the magnitude of the Sr-isotope heterogeneity in the melt inclusions from these two samples is approximately equal to the variability observed in Vailulu'u seamount lavas, although the melt inclusions sample a more depleted component than observed in whole rocks from this seamount. Among the Vailulu'u samples, only sample 71-11 ($^{87}Sr/^{86}Sr=0.70653–0.70692$, $n=2$)

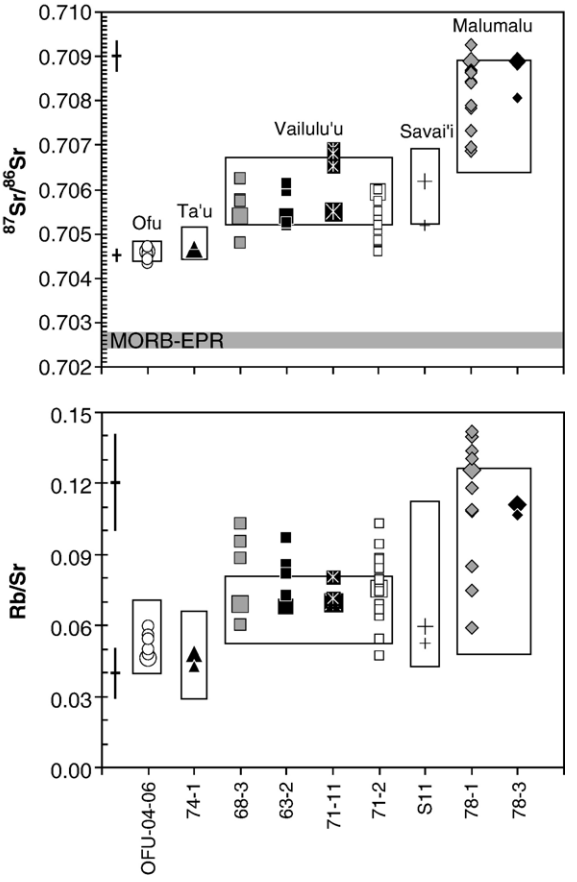

Fig. 1. $^{87}Sr/^{86}Sr$ (upper panel) and Rb/Sr (lower panel) in melt inclusions from nine basalt samples compared to the total variation in each island/seamount (shown by boxes). References for whole-rock data can be found in [4]. The nine whole rocks from which the melt inclusions were separated are represented by larger symbols. No melt inclusions are more isotopically depleted than the most depleted lava measured in the island chain ($^{87}Sr/^{86}Sr>0.7044$). The range for EPR N-MORB [22] (averaged by segment) plots significantly below the Samoan whole rocks and melt inclusions. Replicate analyses on the same melt inclusion are averaged. The Rb/Sr for Savai'i whole-rock sample SAV1-25 is not included because of alteration. Internal precision (2σ, standard error) for $^{87}Sr/^{86}Sr$ is approximately the size of the data symbols. $^{87}Sr/^{86}Sr$ error bars represent error propagated from the Rb correction, as determined on Samoan glass standards, and dominates the error associated with $^{87}Sr/^{86}Sr$ measurement by LA-ICP-MS; maximum and minimum (500 and 150 ppm) errors are shown for reference. Error bars for Rb/Sr are ±17% (2σ, standard deviation), and are based on the reproduceability of Rb/Sr measurement on Samoan glass standards; internal precision for Rb/Sr averages an order of magnitude better. Samples are listed in order of increasing whole-rock $^{87}Sr/^{86}Sr$, from left to right.

hosts inclusions that sample compositions similar to the most enriched isotopic compositions observed in Vailulu'u volcano. Like sample 71-11, isotopic analyses of melt inclusions from sample 63-2 ($^{87}Sr/^{86}Sr$=0.70520–0.70613, n=3) lie completely within the isotopic range found in the whole rocks from Vailulu'u seamount. OFU-04-06 melt inclusions exhibit the least isotopic variability ($^{87}Sr/^{86}Sr$=0.70434–0.70469, n=7) among the samples with isotopic analyses on more than two different inclusions, and this variability is similar to the variability sampled by whole-rock lavas from the island. There is only a single melt inclusion analysis from each of basalt samples 78-3 (0.70807), 74-1 (0.70477) and S11 (0.70518); the Sr-isotope ratios lie within the range observed in the respective host volcanoes.

Although melt inclusions show more depleted isotopic compositions than the island or seamount from which they were recovered, they are not observed to sample compositions more depleted than whole rocks from the Samoan hotspot ($^{87}Sr/^{86}Sr \geq 0.7044$). Therefore, the least radiogenic Sr-isotope ratios in Samoan basalts and melt inclusions are significantly more enriched than the depleted upper mantle sampled by MORB along the EPR (East Pacific Rise; 0.70228–0.70287, N-MORB segment averages from [22]); the old oceanic crust upon which the Samoan island chain is constructed is probably isotopically similar to these modern EPR basalts.

Rb/Sr ratios measured by LA-ICP MS on the same set of melt inclusions tell a story similar to that of the isotopes. Melt inclusions in sample 78-1 exhibit the largest variation in Rb/Sr ratios (0.0593–0.1421), and the variability is similar to that observed in the whole rocks measured from Malumalu seamount. The Rb/Sr ratios in OFU-04-06 melt inclusions show some heterogeneity (Rb/Sr from 0.0476 to 0.0595, n=7), but this variability is smaller than the variability sampled by whole-rock lavas from the island. Vailulu'u melt inclusions from dredge samples 71-2 (Rb/Sr from 0.0469 to 0.1028, n=12 melt inclusions) and 68-3 (Rb/Sr from 0.060 to 0.1027, n=3) exhibit a range of Rb/Sr values that falls between 78-1 and OFU-04-06. Unlike the isotopes, however, the magnitude of the Rb/Sr heterogeneity in the melt inclusions from samples 71-2 and 68-3 is greater than the variability observed in Vailulu'u seamount lavas, and, within error of measurement, do not sample a component with lower Rb/Sr than observed in whole rocks from this seamount.

The present dataset suggests that the isotopic variability exhibited by the melt inclusions in a basalt sample may be a function of the whole-rock isotopic composition. In Fig. 2, the Sr-isotope variability of melt inclusions in three basalt samples–those with the largest number of melt inclusion analyses–is plotted against the bulk $^{87}Sr/^{86}Sr$ composition of the respective whole rocks. The $^{87}Sr/^{86}Sr$ variability, determined by the difference between the highest and the lowest $^{87}Sr/^{86}Sr$

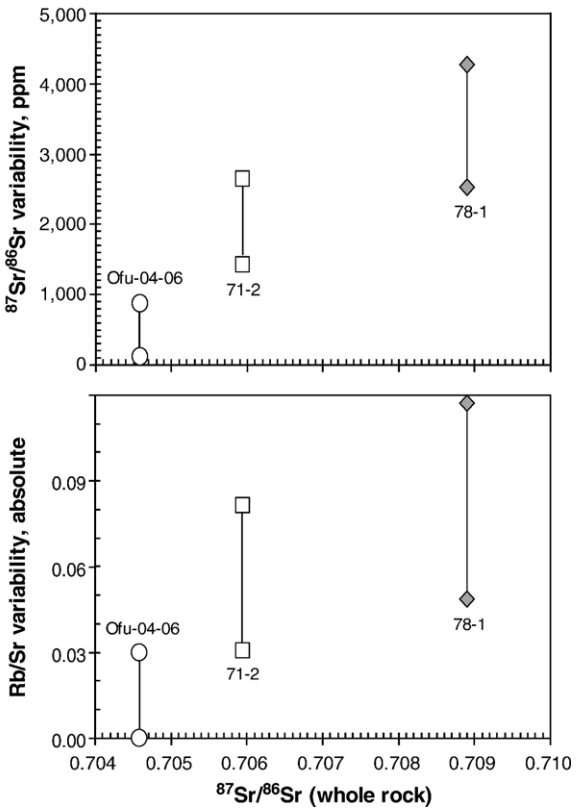

Fig. 2. Upper panel: Melt inclusion isotopic variability (in ppm) as a function of whole-rock $^{87}Sr/^{86}Sr$ ratio for the three Samoan lavas with the greatest number of melt inclusion analyses. Melt inclusion isotopic variability increases with increasing $^{87}Sr/^{86}Sr$ (and decreasing $^{3}He/^{4}He$, not shown) in the three Samoan basalts. Variability is determined by the difference between the most isotopically extreme melt inclusions in a basalt sample. The maximum and minimum values for this variability are a result of the uncertainty introduced by the Rb correction, which is directly related to the Rb/Sr of the melt inclusion. For example, the maximum variability in basalt sample 78-1 is determined by the difference between the highest (0.7092 plus 391 ppm uncertainty) and lowest plausible $^{87}Sr/^{86}Sr$ (0.7072 minus 393 ppm uncertainty). The minimum variability is determined by the difference between the lowest plausible $^{87}Sr/^{86}Sr$ in the most enriched melt inclusion (i.e., 0.7089, or 0.7092 minus 389 ppm uncertainty) and the highest plausible $^{87}Sr/^{86}Sr$ in the most depleted melt inclusion (0.7074, or 0.7072 plus 393 ppm uncertainty). Lower panel: Melt inclusion Rb/Sr variability (absolute) as a function of whole-rock $^{87}Sr/^{86}Sr$ ratio. Maximum and minimum variability is determined the same way, but assumes an uncertainty for Rb/Sr of 17%. The magnitude of variability due to internal precision is approximated by the size of the data symbols in both panels.

ratios from melt inclusions in a given basalt sample, exhibits a maximum and a minimum due to the uncertainty introduced by the Rb correction. Although the number of data points is limited, the data are consistent with melt inclusion isotopic diversity increasing with increasing $^{87}Sr/^{86}Sr$ (increasing EM2 component) and decreasing $^{3}He/^{4}He$ (not shown). The range of variability for Malumalu sample 78-1 is larger than, but overlaps with, the range of values from Vailulu'u sample 71-2. The melt inclusions from the high $^{3}He/^{4}He$ Ofu basalt exhibit the smallest range of probable $^{87}Sr/^{86}Sr$ ratios, and they do not overlap with the range from samples 71-2 and 78-1. A similar observation can be made for the variability of Rb/Sr ratios in the melt inclusions, where Rb/Sr tends toward greater melt inclusion variability in samples 78-1 and 71-2; the Ofu sample has the smallest range of variability, and overlaps slightly with the lowest probable variability in sample 71-2. It is notable that OFU-04-06 exhibits the highest $^{3}He/^{4}He$ ratio (and low $^{87}Sr/^{86}Sr$) found in Samoa, an observation that may be linked to the small degree of isotopic and trace element variability in its melt inclusions.

3.2. Major and trace element characteristics of melt inclusions

Rb/Sr and $^{87}Sr/^{86}Sr$ ratios from the melt inclusions define a broad array that encompasses the entire spectrum of Sr-isotope and Rb/Sr variability recorded in Samoan basalts (Fig. 3). Curiously, the melt inclusions from Malumalu do not form an array by themselves, but plot over a broad region. The Rb/Sr and Sr-isotope data array form a crude mantle isochron of 1.1 Ga.

Major and trace elements were measured on melt inclusions from Vailulu'u, Malumalu and Ofu basalts, and they reveal a large range of compositions (Table 2). Although the trace element compositions of Vailulu'u melt inclusions are similar to whole-rock analyses from this seamount, melt inclusions from EM2 endmember basalt 78-1 record a greater degree of trace element variability than all of the whole rocks measured from Malumalu. One

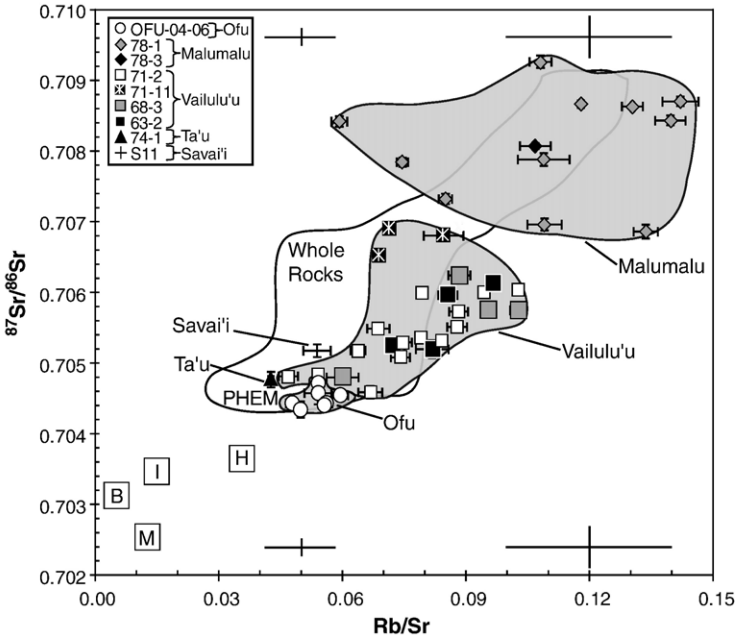

Fig. 3. $^{87}Sr/^{86}Sr$ versus Rb/Sr ratios for Samoan whole rocks and melt inclusions, determined by laser ablation. The shaded regions represent the extent of melt inclusion variability for the volcanoes (Vailulu'u, Malumalu and Ofu). The open region encompasses the least evolved ($MgO \geq 6.5$ wt.%) whole-rock measurements from these three volcanoes and Ta'u, thus encompassing islands and seamounts only on the eastern half of the Samoan hotspot track (where ~98% of the analyzed melt inclusions were recovered). Whole-rock data from Ofu is unpublished, and for the other volcanoes is from [4]. MORB range is limited to EPR N-MORB (M) segment averages [22]. High $^{3}He/^{4}He$ basalts from Hawaii (H) [37], Iceland (I) [38] and Baffin Island (B) [39] provide an approximation for FOZO (higher $^{3}He/^{4}He$ ratios exist for Hawaiian basalts [40], but $^{87}Sr/^{86}Sr$ data are not available for these samples; Rb/Sr data for high $^{3}He/^{4}He$ samples from Baffin Island are found in [41]). Error bars on symbols are internal precision of measurement (2σ, mean deviation). Error bars on periphery of figure denote external precision of measurements, as determined by Samoan glass standards with compositions similar to the melt inclusions: Rb/Sr error is 17% (2σ, standard deviation) and $^{87}Sr/^{86}Sr$ error is based on error associated with the Rb correction (2σ, standard deviation). Replicate analyses of the same melt inclusion are shown. The melt inclusion data form a crude mantle isochron age of ~1.1 Ga.

Table 2
Melt inclusion major and trace element data (uncorrected for olivine fractionation), and host olivine composition

Sample #	Disc #	Grain #	SiO_2	TiO_2	Al_2O_3	FeO	MnO	MgO	CaO	Na_2O	K_2O	P_2O_5	Total	Mg #	OlFo	Rb	Sr	Y	Zr	Nb	Ba	La	$^{87}Sr/^{86}Sr$ [a]	Type
78-1	Disc1	#7	45.64	3.77	12.97	14.11	0.14	6.85	9.53	3.46	2.16	0.46	99.19	49.0	84.6	181	1176	83.6	979	–	–	–	0.70926	H
78-1	Disc1	#9	46.57	2.99	13.06	10.75	0.16	8.02	13.09	2.94	1.57	0.44	99.74	59.6	84.4	49	443	33.0	245	–	–	45.6	0.70732	H
78-1	Disc1	#10–11	44.98	3.22	12.84	11.18	0.14	9.26	11.29	2.62	1.76	0.39	98.10	62.1	84.0	75	507	28.1	269	–	–	–	–	H
78-1	Disc1	#12	46.37	3.76	13.09	11.51	0.17	8.03	11.38	2.93	1.91	0.40	99.65	58.0	84.4	59	545	33.2	339	73.1	390	–	–	H
78-1	Disc2	#5	45.16	3.42	12.62	11.09	0.17	9.15	12.42	2.46	1.42	0.42	98.68	62.0	84.3	130	1127	75.5	568	132.9	796	96.1	–	H
78-1	Disc2	#6	47.22	3.45	13.60	11.80	0.23	7.10	10.17	3.13	2.10	0.42	99.38	54.4	83.6	115	926	54.1	543	122.4	666	93.8	0.70843	H
78-1	Disc2	#7	47.20	2.92	13.65	9.94	0.14	7.83	11.36	2.73	2.00	0.40	98.49	60.9	83.9	–	–	–	–	–	–	–	–	H
78-1	Disc2	#8	45.57	3.20	12.26	11.20	0.17	9.26	11.33	2.71	1.33	0.47	97.88	62.1	83.6	71	679	40.6	360	76.0	409	57.7	–	H
78-1	Disc2	#9	46.81	3.46	14.03	11.81	0.16	7.34	10.54	2.93	1.91	0.43	99.59	55.2	82.8	76	655	38.7	400	84.8	482	72.3	0.70870	H
78-1	Disc2	#10	46.32	3.46	13.16	11.01	0.15	7.65	11.60	4.80	1.27	0.46	100.01	57.9	83.6	33	631	37.3	346	73.4	450	65.1	0.70842	H
78-1	Disc2	#11Le	46.32	3.24	12.74	11.04	0.14	8.18	12.72	3.18	1.33	0.39	99.67	59.5	83.6	55	598	36.7	281	56.1	401	45.5	–	H
78-1	Disc2	#11RtS	–	–	–	–	–	–	–	–	–	–	–	–	83.2	194	1694	100.5	871	193.5	1258	173.6	–	H
78-1	Disc2	#11RtL	44.61	3.77	12.99	11.76	0.19	6.23	13.20	2.70	1.57	0.44	97.85	51.2	83.2	299	2480	158.7	1310	293.5	1887	246.6	–	H
78-1	Disc2	#3	46.09	3.23	12.50	10.68	0.15	8.85	11.47	2.59	1.59	0.43	97.91	62.1	84.1	135	1038	62.5	579	126.8	719	100.6	–	H
78-1	Disc2	#4	46.45	2.99	12.17	10.32	0.15	9.22	12.92	2.37	1.37	0.40	98.80	63.9	83.9	104	901	55.1	465	110.9	686	78.9	–	H
78-1	Disc3	#4	46.07	3.81	13.22	10.47	0.12	6.00	12.52	2.93	1.80	0.42	97.81	53.1	85.2	69	555	26.4	297	64.8	370	55.4	0.70866	G
71-2	Disc1	g#3–4	48.50	2.66	12.55	9.41	0.14	7.38	14.63	2.33	0.84	0.35	99.13	60.8	87.4	26	384	23.0	185	30.4	124	22.4	–	G
71-2	Disc1	i	48.13	2.57	12.54	9.21	0.14	8.07	13.85	2.48	0.78	0.27	98.40	63.4	90.7	–	–	–	–	–	–	–	0.70602	G
71-2	Disc3	#3	46.12	3.48	13.06	10.94	0.15	5.81	14.09	2.55	1.29	0.32	98.23	51.3	84.3	50	517	29.5	237	52.7	347	40.9	–	G
71-2	Disc3	#5	46.71	3.10	12.72	9.66	0.15	7.90	13.10	2.45	1.24	0.32	97.72	61.8	91.0	45	504	27.1	243	58.8	314	35.3	0.70534	G
71-2	Disc3	#6	46.46	3.23	12.31	10.52	0.17	7.54	13.64	2.64	1.14	0.36	98.50	58.7	85.7	50	579	33.3	281	60.1	342	49.9	0.70599	G
71-2	Disc3	C	48.87	3.33	13.16	8.77	0.15	7.63	12.81	2.68	0.83	0.39	98.94	63.3	88.8	27	437	22.2	232	42.6	177	33.9	0.70482	G
71-11	Disc3	#1	49.01	3.13	12.53	11.05	0.18	6.15	12.01	2.85	0.94	0.40	98.51	52.4	81.4	34	419	27.1	232	41.4	205	35.6	0.70680	G
71-11	Disc1	a	49.28	2.82	12.70	10.94	0.14	6.89	11.63	2.60	1.01	0.37	98.73	55.5	83.0	36	409	30.3	223	40.9	214	33.0	0.70672	G
68-3	Disc1	#6mi1	48.77	2.88	14.30	8.75	0.13	4.68	14.74	2.64	1.35	0.37	98.98	51.4	87.9	54	533	27.0	260	62.5	378	46.3	0.70624	G
OFU-04-06	Ofu	13	44.25	3.31	12.60	10.10	0.11	7.99	13.38	3.40	0.94	0.50	96.75	61.4	79.8	52	856	41.6	464	76.8	343	106.2	0.70457	H
OFU-04-06	Ofu	14	46.33	3.07	14.03	8.64	0.07	8.03	11.89	3.52	1.08	0.53	97.24	54.9	80.4	61	613	33.3	352	55.6	311	77.8	–	H
OFU-04-06	Ofu	15	46.47	2.81	13.67	10.58	0.14	7.20	10.64	3.96	1.09	0.33	96.96	60.5	77.3	60	700	30.0	374	54.8	303	82.1	0.70443	H
OFU-04-06	Ofu	16	46.74	3.13	14.12	7.00	0.09	8.26	13.11	3.76	1.19	0.45	97.97	49.5	81.9	68	760	38.6	393	72.5	363	91.1	–	H
OFU-04-06	Ofu	18	50.44	1.16	14.17	7.56	0.07	7.33	11.22	4.69	1.38	0.39	98.67	51.4	79.3	63	926	33.8	460	84.1	399	113.9	–	H
OFU-04-06	Ofu	19	47.15	2.14	11.15	17.06	0.21	13.83	2.72	1.56	1.71	0.46	98.00	75.2	76.6	–	–	–	–	–	–	–	–	H
OFU-04-06	Ofu	20	47.36	2.90	14.50	9.00	0.13	7.59	10.84	4.02	1.06	0.39	97.84	55.1	78.6	81	909	39.0	438	70.3	402	32.5	–	H
OFU-04-06	Ofu	24rep	46.35	3.58	13.47	8.58	0.09	8.11	13.70	3.23	0.72	0.29	98.13	55.8	83.0	–	–	–	–	–	–	–	–	H
OFU-04-06	Ofu	25	45.74	3.16	13.55	11.98	0.12	7.71	11.15	3.54	0.89	0.42	98.33	63.6	77.2	59	659	38.1	383	48.7	243	–	0.70454	H
OFU-04-06	Ofu	26	46.14	2.51	12.70	10.60	0.10	8.04	13.61	3.01	0.74	0.34	97.93	62.3	76.5	45	573	37.7	338	42.3	191	–	0.70443	H

OFU-04-06	Ofu	27	44.62	3.36	13.38	10.12	0.10	7.99	12.36	3.35	0.91	0.49	96.82	60.0	79.5	55	807	40.2	457	75.8	321	111.4	–		H
OFU-04-06	Ofu	28	47.60	2.70	13.87	9.87	0.08	7.49	10.92	4.18	0.94	0.33	98.13	58.5	78.4	58	744	34.6	382	71.1	322	94.3	0.70434		H
OFU-04-06	Ofu	30	47.23	3.03	13.82	7.23	0.09	7.78	12.39	3.74	1.15	0.24	96.79	50.9	82.3	63	634	32.8	324	54.0	283	76.6	–		H
OFU-04-06	Ofu	31	42.22	2.01	13.18	14.43	0.12	7.24	12.41	4.17	1.14	0.43	97.95	68.4	80.3	87	1006	46.6	515	79.4	445	136.2	–		H
OFU-04-06	Ofu	33	41.65	2.83	13.21	16.38	0.17	6.96	10.68	3.77	1.06	0.34	97.17	71.1	77.7	66	961	39.1	479	81.9	391	105.9	–		H
OFU-04-06	Ofu	2	46.18	3.00	13.70	9.93	0.13	7.53	11.26	3.70	0.99	0.32	96.80	58.9	76.5	50	800	35.5	409	81.5	326	80.9	0.70469		H
OFU-04-06	Ofu	3	45.75	3.12	13.20	7.91	0.10	8.20	13.67	3.01	0.83	0.37	96.24	54.3	83.8	41	714	36.8	398	72.2	301	72.4	0.70443		H
OFU-04-06	Ofu	4	45.71	3.05	13.40	10.95	0.06	7.62	10.88	3.93	0.93	0.33	96.89	61.8	77.2	56	772	33.6	420	73.2	326	70.2	–		H
OFU-04-06	Ofu	5	47.03	3.01	14.37	8.75	0.12	7.66	11.77	3.70	1.21	0.19	97.92	54.7	81.4	79	661	31.6	333	63.5	393	78.9	–		H
OFU-04-06	Ofu	8	45.83	3.21	13.50	10.96	0.13	7.74	11.19	4.06	0.98	0.36	98.04	61.6	77.7	63	861	40.0	462	81.2	363	102.5	–		H
OFU-04-06	Ofu	9	44.84	3.37	13.52	12.21	0.15	6.89	10.62	4.25	1.04	0.32	97.31	64.1	77.4	77	1006	42.7	528	98.4	444	104.7	–		H
OFU-04-06	Ofu	22	38.04	4.65	10.75	12.83	0.18	9.84	17.18	1.15	0.12	0.59	95.55	70.3	80.9	18	1161	72.4	821	121.9	255	38.9	–		H
OFU-04-06	Ofu	21	45.30	4.63	14.07	10.83	0.20	6.89	9.58	4.35	1.57	0.74	98.40	60.4	78.1	67	779	34.8	417	51.7	271	51.4	–		H
OFU-04-06	Ofu	23	45.58	5.87	12.35	8.58	0.12	8.17	13.00	3.71	1.32	0.84	99.47	57.9	80.6	85	1042	48.6	551	78.9	374	38.4	–		H
OFU-04-06	Ofu	7(fir)	–	–	–	–	–	–	–	–	–	–	–	–	–	110	894	21.2	289	112.8	588	97.6	–		H
OFU-04-06	Ofu	7(sec)	–	–	–	–	–	–	–	–	–	–	–	–	–	65	809	37.5	428	74.1	365	104.7	–		H

Rb/Sr ratios by LA-ICP-MS are considered to be more accurate than those obtained by ion probe. Any discrepancy between the Rb/Sr ratios measured by the two methods is probably due to the difficulty of measuring Rb by ion probe techniques. Samples 78-1, 71-2, 71-11 and 68-3 are from the Samoan AVON3 dredging cruise, and their sample names are preceded by the prefix "AVON3."
Major element data are in wt.%, and trace elements are in ppm. Forsterite contents of the host olivines (Ol Fo) are also given. Glassy (G) or Homogenized (H).

[a] See data in Table 1 for Sr-isotope data.

melt inclusion from sample 78-1 displays high Sr and Ba concentrations (2500 and 1900 ppm, respectively) that are 6 times more enriched than any whole-rock lavas examined from Malumalu. This ultra-enriched composition is significantly more enriched than observed in any Samoan basalts, and is derived from either an extremely enriched source or from very small degrees of melting.

Melt inclusions from OFU-04-06 also exhibit some unusual major and trace element compositions. One Ofu melt inclusion exhibits unusually low K_2O concentrations. Additionally, the OFU-04-06 melt inclusions exhibit a large range in SiO_2, including one sample with unusually low SiO_2 (38.0%) and high CaO (17.2%). These uncommon major element compositions may be due to the combination of unusual phases present in the OFU-04-06 melt inclusions prior to homogenization in the lab. Low glass totals in the OFU-04-06 inclusions are likely due to high volatile contents in the homogenized glasses, a hypothesis consistent with the volatile-rich phases in melt inclusions from this sample.

In addition to Rb/Sr ratios, several other major and trace element parameters correlate with $^{87}Sr/^{86}Sr$ in the melt inclusions. Melt inclusions from Ofu, Vailulu'u and Malumalu exhibit negative Ba anomalies that also are observed in Samoan shield-stage lavas [4] (Fig. 4). An approximation for this Ba anomaly is $(Ba/Nb)_N$ (normalized to PUM, primitive upper mantle [30]), a ratio which correlates with $^{87}Sr/^{86}Sr$ in whole rocks and melt inclusions (Fig. 5). The $(Ba/Nb)_N$ values are lowest (largest Ba-anomaly) in the basalts and melt inclusions with low $^{87}Sr/^{86}Sr$, and highest in the basalts and melt inclusions with elevated $^{87}Sr/^{86}Sr$ ratios. It is notable that basalts and melt inclusions associated with elevated $^3He/^4He$ ratios, and not the high $^{87}Sr/^{86}Sr$ EM2 end-member basalts, have the largest Ba anomalies. The mechanism that generates this anomaly is unknown [4], and the anomaly also exists in MORB and HIMU basalts, but not in basalts with EM1 characteristics.

The negative K_2O anomaly in the Samoan melt inclusions (Fig. 4) is commonly observed in OIBs. Curiously, however, PUM-normalized K exhibits little variability regardless of the degree of enrichment of the other trace elements (with the exception of a single Ofu melt inclusion). Despite the limited variability, olivine fractionation-corrected K_2O concentrations exhibit a relationship with $^{87}Sr/^{86}Sr$ in the melt inclusions (Fig. 5).

Nb/Zr also correlates with $^{87}Sr/^{86}Sr$ in Samoan basalts and melt inclusions (Fig. 5). The lowest Nb/Zr ratios are associated with unradiogenic $^{87}Sr/^{86}Sr$ values. Nb/Zr ratios correlate with Pb-isotopes [4] and inversely with $^3He/$

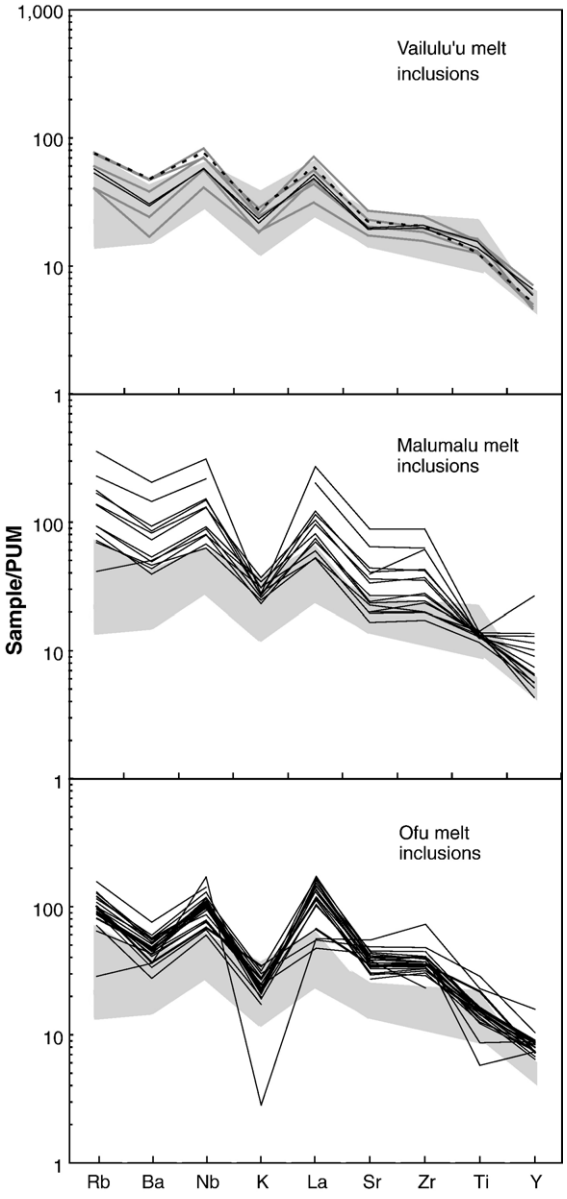

Fig. 4. PUM-normalized trace element patterns of Samoan basalts and melt inclusions; melt inclusion data is from ion probe analysis, except for K and Ti, which were measured by electron probe. Vailulu'u melt inclusions are from three samples: 71-2 (grey lines), 68-3 (dashed line), 71-11 (solid black lines). Malumalu and Ofu melt inclusions are from samples 78-1 and OFU-04-06, respectively. All melt inclusions (except for one melt inclusion from 78-1 and two from OFU-04-06 that have no major element compositions, see Table 2) are corrected for olivine fractionation to be in equilibrium with mantle olivine of Fo_{90} (see text for correction scheme). The grey field encloses the range of whole-rock patterns from the least evolved basalts (>6.5 wt.% MgO) from Vailulu'u, Ofu and Malumalu; whole-rock compositions have been corrected for olivine addition/fractionation. PUM values from [30].

^{4}He (not shown) in Samoan basalts. Nb/Zr may serve as a proxy for ^{3}He/^{4}He isotopes in Samoan melt inclusions; therefore, it may be important that the Nb/Zr ratios in several of the Ofu-04-06 melt inclusions exhibit values lower than the ratios observed in whole rocks.

3.3. Melting models of the EM2 source

It is important to place constraints on the trace element variability introduced by melting processes. A plot of Sr versus Ti/Zr shows that the majority of the melt inclusions form an array that extends outside of the whole-rock field to enriched Sr and low Ti/Zr values (Fig. 6). The low Ti/Zr ratios (15-88) observed in the melt inclusions extend to lower values than observed in whole-rock basalts from the eastern Samoa islands and seamounts (63-130). Such low values cannot be produced by crystal fractionation of melts before olivine entrapment, and assimilation of MORB (Ti/Zr=88) also fails to produce low Ti/Zr values [31]. A model of the Samoan EM2 source composition [4] provides a robust estimate for the mantle source sampled by the extreme EM2 basalt sample 78-1, and variable degrees of aggregated modal fractional melts of this source (Sr=20.0 ppm, Ti/Zr=101.9) in the garnet and spinel stability fields can describe much of the melt inclusion array in Fig. 6. Consistent with the model of the EM2 source as a metasomatized harzburgite [4], we adopt a harzburgite source lithology (1% spinel, 3.6% clinopyroxene [cpx], 20.6% orthopyroxene [opx] and 74.8% olivine), with mineral modes from [32] and mineral/melt partition coefficients from [33]. We assume the mineral modes of a similar bulk composition for melting in the garnet stability field (3.8% garnet, 2.7% cpx, 17.7% opx and 75.8% olivine) using the spinel to garnet conversion from [34]. The two melting models follow similar trajectories, but melting in the spinel stability field is required to generate the exceptionally high Sr and low Ti/Zr observed in the ultra-enriched Malumalu melt inclusions. Interestingly, if the EM2 source [4] has a more cpx-rich lithology than the harzburgite in our melting model, it will not produce melts with the Sr concentrations observed in the most enriched melt inclusion at reasonable degrees (>1%) of melting (Fig. 7).

Other geochemical indicators, including Y/Zr ratios, more clearly resolve the relative roles of melting in the garnet and spinel stability fields. Due to the relative compatibility of Y in residual garnet, low Y/Zr ratios are consistent with melting in the presence of garnet. A role for melting in the garnet stability field is suggested in a plot of Y/Zr against Nb/Zr in Fig. 6. This is particularly true for the Ofu melt inclusions, which trend to the lowest Y/Zr ratios

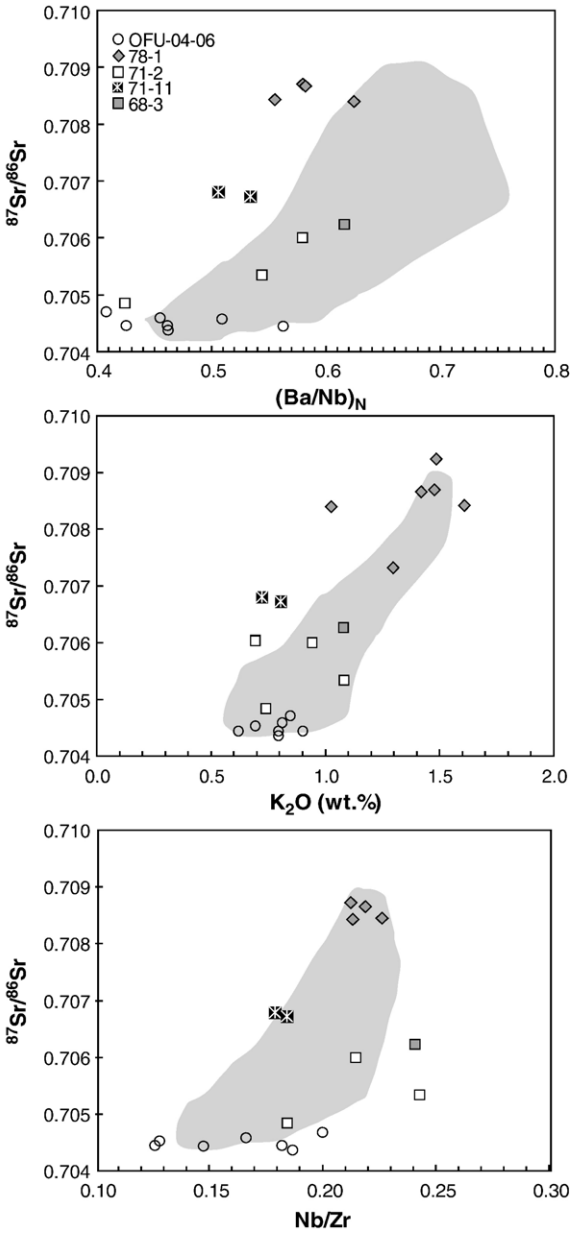

Fig. 5. Nb/Zr, K_2O and Ba/Nb_N versus $^{87}Sr/^{86}Sr$. K_2O measured by electron probe, and Nb, Zr and Ba by ion probe. $(Ba/Nb)_N$ (normalized to PUM) is used as a proxy for the pervasive negative Ba anomaly in Samoan shield-stage basalts. The EM2 basalts and melt inclusions are associated with elevated Nb/Zr, K_2O and $(Ba/Nb)_N$ (smaller negative Ba anomalies), and the low $^{87}Sr/^{86}Sr$ basalts exhibit lower Nb/Zr, K_2O and $(Ba/Nb)_N$ (larger negative Ba anomalies). All melt inclusions are corrected for olivine fractionation. The grey fields enclose the range of whole-rock patterns from the least evolved basalts (>6.5 wt.% MgO) from Vailulu'u, Ofu and Malumalu (whole-rock compositions have been corrected for olivine addition/fractionation). Symbols are the same as Fig. 3. $^{87}Sr/^{86}Sr$ internal precision (2σ, standard error) is approximately the size of the symbol.

observed in the melt inclusions suite and straddle the garnet melting trend at 5% melt. This is similar to the Ti/Zr versus Sr plot, where the garnet melting curve trends through the Ofu melt inclusion field at ~4% melt. Malumalu and Vailulu'u melt inclusions (and Samoan whole rocks) are offset to higher Y/Zr ratios, perhaps suggesting a larger role for melting in the spinel stability field, an observation that is consistent with the same subset of melt inclusions in the Ti/Zr versus Sr melt model.

No single melting model of the EM2 source perfectly describes the melt inclusion fields for all three volcanoes, but we find that a combination of melting and mixing satisfactorily reproduces the melt inclusion geochemical variability. The relative roles of melting and mixing of different components can be partially deconvolved in a plot of $^{87}Sr/^{86}Sr$ versus 1/Sr (Fig. 8), where two-component mixing trajectories are linear and variable degrees of melting result in horizontal trajectories. The Ofu melt inclusions lie on a horizontal trend, which can be described by various degrees of melting of a single source that exhibits a $^{87}Sr/^{86}Sr$ ratio of ~0.7045, and the Malumalu and Vailulu'u melt inclusions form a diagonal array that suggests a role for two-component mixing.

4. Discussion

4.1. A homogeneous source for PHEM basalts

Compelling evidence that the Samoan melt inclusions sample a heterogeneous source comes from Sr-isotope analysis of the melt inclusions from Vailulu'u and Malumalu basalts. However, the uniformly unradiogenic character of the Ofu melt inclusions precludes a significant contribution from an enriched, radiogenic (EM2) component. This suggests that Samoan melts with high $^3He/^4He$ sample a homogeneous source and do not mix with melts of an enriched component. By comparison, the melt inclusions from Malumalu and Vailulu'u span a large range of Sr concentrations and isotopic compositions, indicating that both variable degrees of melting and mixing have occurred. An aggregated fractional melt trajectory for the garnet stability field is plotted (Fig. 8) for the EM2 source [4], and the Malumalu and Vailulu'u melt inclusions form a broad array that trends diagonally away from the horizontal Ofu melting trajectory toward low degree (~1%) melts of the EM2 source; the Vailulu'u and Malumalu melt inclusions can be produced by aggregated melts of an Ofu source that then mix with aggregated fractional garnet melts of the EM2 source.

Unlike the EM2 source, the trace element source composition of the high $^3He/^4He$, lower $^{87}Sr/^{86}Sr$ Ofu source component is less clear. Called PHEM [23], this

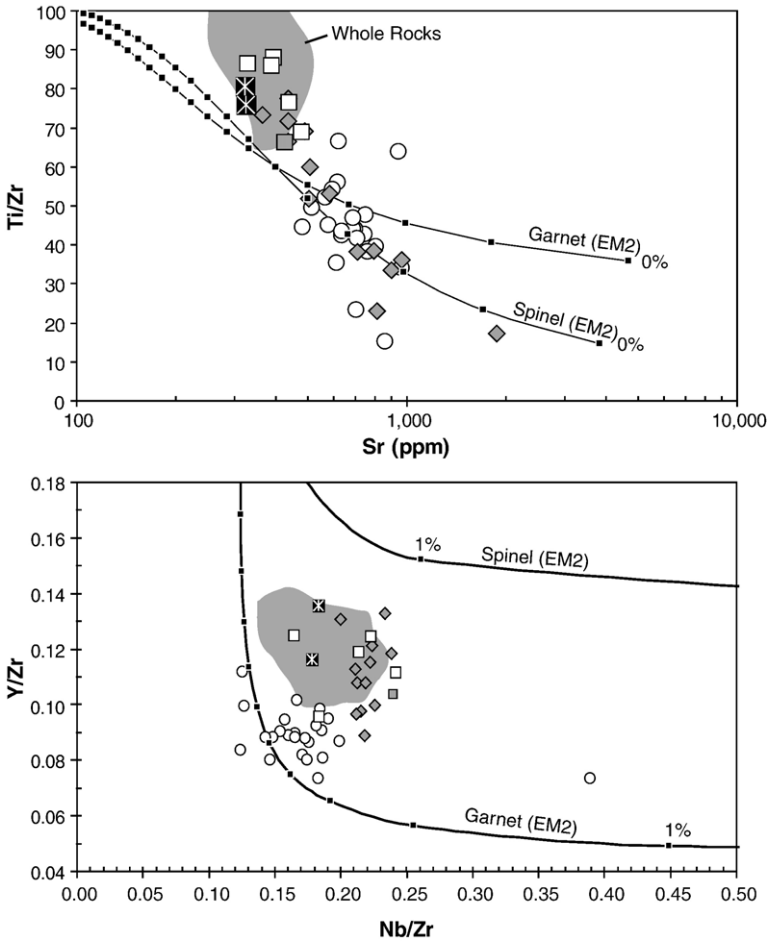

Fig. 6. Upper panel: Ti/Zr versus Sr concentration in melt inclusions and whole rocks with melting models. All melt inclusions and whole rocks are corrected for olivine fractionation to be in equilibrium with mantle olivine. Grey field is for whole-rock samples from Vailulu'u, Malumalu and Ofu. Lines with closed boxes represent aggregated fractional melting trends of the EM2 source [4] in the garnet and spinel stability fields, using partition coefficients from [33]. Harzburgite mineral modes are from [32]. All melting is non-modal. Tick marks are every 1% melting, beginning at 0% and increasing to the left. Lower panel: Y/Zr versus Nb/Zr in melt inclusions and whole rock, including melting models in the garnet and spinel stability fields. Tick marks are every 1% and the degree of melting increases to the left. Melting parameters and grey field are the same as upper panel.

component melts to form basalts and melt inclusions from Ofu. However, it is possible to bracket the source composition of this component and estimate the degree of melting captured in the Ofu melt inclusions. Although the Ofu basalts are more isotopically depleted than the EM2 basalts, an isotopically and trace element depleted DMM lherzolite source (7 ppm Sr) [35] fails to produce the high Sr concentrations observed in the Ofu melt inclusions (Fig. 7). This would suggest that the Ofu source is either more refractory or more trace element enriched, or both, than the lherzolitic [35] DMM source. The first option can be explored by invoking a more refractory, harzburgitic DMM source. However, only unreasonably low ($F<1\%$) degrees of melting can produce the most enriched Sr concentration observed an Ofu melt inclusion. The second scenario can be tested by invoking the trace element enriched EM2 source, and assigning it a lherzolitic lithology that is similar to DMM. At reasonable degrees of melting ($F=1.5\%$), such a source can generate melts with sufficiently high Sr contents to match the range observed in Ofu. Finally, a harzburgitic EM2 source, which is both more refractory and trace element enriched than DMM, can generate the most enriched melt inclusions from Malumalu and Ofu between 1% and 2% melting. The harzburgitic EM2 source can serve as a probable upper limit for the trace element enrichment of the PHEM source because we consider it unlikely for the less isotopically enriched PHEM component to exhibit greater trace element enrichment than EM2. However,

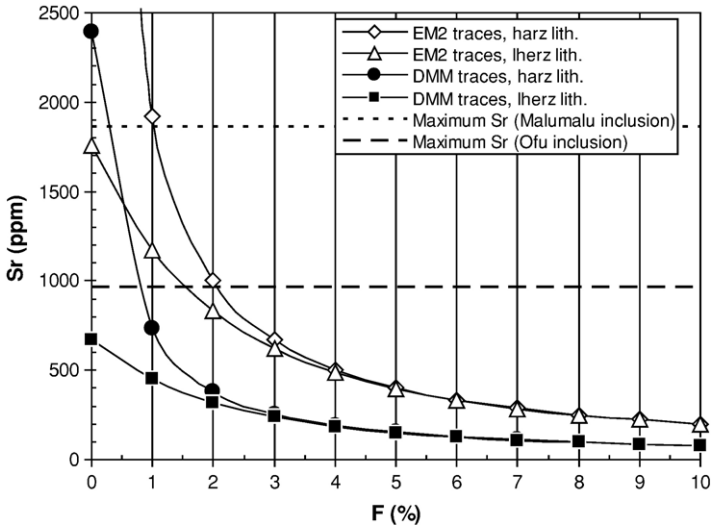

Fig. 7. Sr in melt versus degree of melting (F) for various combinations of two lithologies and two trace element source abundances. Two dashed lines represent olivine fractionation-corrected Sr concentrations in the most enriched melt inclusions from Malumalu sample 78-1 (upper line) and Vailulu'u sample 71-2 (lower line). DMM trace element source and lherzolite lithology from [35], converted to equivalent garnet facies lithology using relationship from [34]. EM2 source from [4]. Harzburgite lithology from [32]. Note that only the EM2 source with a harzburgite lithology can produce the highest Sr concentration observed in the melt inclusion from sample 78-1 at $F \geq 1\%$. All melting is non-modal in the garnet stability field. Neither modal melting nor melting in the spinel stability field significantly changes our conclusions at $F \geq 1\%$.

a PHEM source with a lithology (and/or Sr concentrations) intermediate between DMM and EM2 cannot be ruled out. If PHEM has the same Sr content and lithology as the EM2 source, the Vailulu'u and Malumalu melt inclusion arrays can be explained as mixtures of 6.5±1.5% melts of PHEM and ~1% melts of EM2. However, the degree of melting of the PHEM source that contributes to the Malumalu–Vailulu'u mixing array should be taken as a maximum.

Unlike the Ofu melt inclusions, which sample a pure PHEM source, no melt inclusions sample a pure EM2 melt (as calclulated by [4], using ultra-enriched Sr-isotope compositions from Samoan xenoliths [36]). Mixing lines in Fig. 8 between a 1% EM2 melt and 6.5±1.5% PHEM melts indicate that the subset of Vailulu'u and Malumalu melt inclusions with both $^{87}Sr/^{86}Sr$ and Sr concentration data are dominated by a PHEM component, and exhibit less than a ~30% contribution from the EM2 component. However, one Malumalu melt inclusion exhibits a much larger contribution from an EM2 component, as indicated by its high (~1865 ppm) Sr content and low (~17) Ti/Zr ratio (Fig. 6). The PHEM–EM2 melt mixing lines in Fig. 8 suggest that this melt inclusion contains more than a 70% contribution from the EM2 melt component. The mixing model suggests that a 70% contribution from an EM2 melt would produce an extrapolated $^{87}Sr/^{86}Sr$ ratio of ~0.712, which is a significantly higher ratio than has been observed in a Samoan basalt, but close to the $^{87}Sr/^{86}Sr$ of cpx in metasomatized xenoliths from Savai'i in western Samoa. Unfortunately, this ultra-enriched melt inclusion was too small for isotopic analysis.

4.2. Isotopic variability in Samoan melt inclusions: MORB or FOZO?

Correlations between trace elements and Sr isotopes suggest that trace element variability in Samoan basalts and melt inclusions may reflect heterogeneity in the Samoan mantle. Rb/Sr, K_2O, $(Ba/Nb)_N$ and Nb/Zr ratios correlate with Sr isotopes in Samoan lavas and melt inclusions, suggesting that these trace elements are heterogeneous in the Samoan mantle source. However, a combination of melting processes and variable source lithology may drive the observed correlations, limiting the role for source heterogeneity. For example, the relatively constant K_2O concentrations and negative (PUM-normalized) anomalies in Samoan lavas may be a result of residual phlogopite, which may cause K_2O to behave more compatibly in the Samoan source during melting. However, K_2O correlates with $^{87}Sr/^{86}Sr$ in the whole rocks and melt inclusions (Fig. 5), suggesting a role for K_2O heterogeneity in the Samoan source, and that K_2O concentrations in Samoan basalts and melt inclusions may be controlled only partially by melting processes.

Assuming that Rb/Sr variability in Samoan melts reflects source variability, the array formed by the $^{87}Sr/$

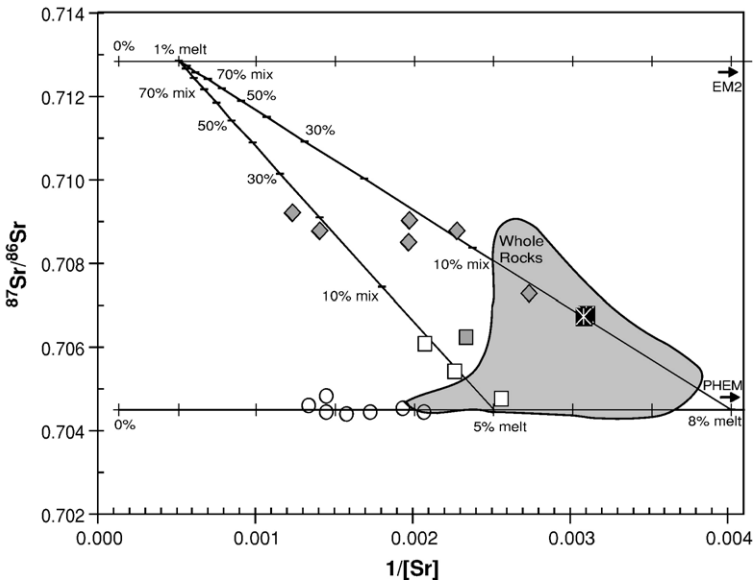

Fig. 8. $^{87}Sr/^{86}Sr$ versus 1/[Sr] for Samoan melt inclusions and basalts. Malumalu and Vailulu'u melt inclusions form a quasi-linear array extending away from the whole-rock basalts from Malumalu, Ofu and Vailulu'u (grey field, same as Fig. 6). Ofu melt inclusions fall off this array, plotting at lower $^{87}Sr/^{86}Sr$ at a given Sr concentration. Aggregated non-modal fractional melting trends of the EM2 and PHEM sources in the garnet stability field are shown as horizontal lines (tick marks are every 1% melting, beginning at 0% and increasing to the right). Two mixing lines, both extending diagonally from a 1% EM2 melt to 5% and 8% PHEM melts, are shown (each tick represents 10% mixture, starting at 0% EM2 and increasing to the upper left). Ofu melt inclusions lie on the melting trend for PHEM, and require no mixing with an EM2 component. Malumalu and Vailulu'u melt inclusions can be described by mixing of melts from the EM2 and PHEM sources. Sr concentrations in melt inclusions and whole rocks are corrected for olivine fractionation. PHEM and EM2 source compositions plot outside of the figure as indicated, at 1/Sr values of ~0.05 (Sr concentrations of 20.0 ppm). The published source for EM2 [4] is used in this figure. As a limit, PHEM is given the trace element source abundances and lithology of EM2 in the melt model. Symbols same as in Fig. 3.

^{86}Sr and Rb/Sr data can be modeled as binary mixing between a PHEM and an EM2 component, a model originally proposed by Farley et al. [23]. Such a model is consistent with the trace element melting/mixing model proposed above, which suggests that the Ofu melt inclusions sample only a high $^{3}He/^{4}He$ PHEM mantle reservoir and the Vailulu'u and Malumalu melt inclusions result from mixing melts from both the PHEM and EM2 mantle reservoirs.

Previous work on the Pb-isotopic variability in melt inclusions [17] suggested that the unradiogenic end-member in EM2 basalts from Tahaa may be depleted (MORB or FOZO?), and thus lie at even lower $^{87}Sr/^{86}Sr$ values than observed in the high $^{3}He/^{4}He$ PHEM lavas from Ofu (Fig. 3). In fact, an extrapolation of the Samoa melt inclusion and whole-rock basalt array in Fig. 3 does indeed trend toward one of two depleted components that are significantly less radiogenic than PHEM: MORB [22] or a common high $^{3}He/^{4}He$ mantle component, called FOZO [24] (Fig. 3). The FOZO component is represented by basalts with the highest $^{3}He/^{4}He$ from Hawaii [37], Iceland [38] and Baffin Island [39]. Both MORB and FOZO lie on a similar extension of the Samoa melt inclusion $^{87}Sr/^{86}Sr$–Rb/Sr array, so it is difficult to distinguish which, if either, of these two components is sampled by the Samoan melt inclusions. If the depleted component is MORB, it may be entrained in melt inclusions by shallow anatexis due to preferential cooling and olivine crystallization near magma chamber and conduit walls [7,8,21]. However, the presence of FOZO (or any other high $^{3}He/^{4}He$ component) in the Samoan melt inclusions would require that the isotopic variability in melt inclusions reflect true source heterogeneity, assuming that a high $^{3}He/^{4}He$ component does not exist in the oceanic crust or lithosphere.

4.3. The case against MORB

It may be possible to look at other lines of geochemical evidence to discern whether MORB or FOZO play a role in augmenting the isotopic diversity in Samoan melt inclusions. Models suggesting that melt inclusion isotopic variability is caused only by contamination from unradiogenic oceanic crust and lithosphere at shallow levels do not explain how several Samoan melt inclusions have higher $^{87}Sr/^{86}Sr$ ratios than their host

bulk rock compositions (see Fig. 1). For example, Samoan whole-rock basalt sample 71-11 hosts several melt inclusions that have $^{87}Sr/^{86}Sr$ ratios (up to 0.70692) that are significantly more enriched than its host rock (0.70550). The presence of $^{87}Sr/^{86}Sr$ ratios in melt inclusions that are higher than the bulk rock require that at least some of the isotopic variability present in melt inclusions is derived from the mantle source, because the enriched component in melt inclusion 71-11a is too enriched to be found in the oceanic crust and lithosphere. Therefore, if assimilation of oceanic crust and lithosphere contributes heterogeneity to the Samoan melt inclusions, it cannot be the only means by which isotopic heterogeneity is produced in Samoan melt inclusions, and some contribution from the melt source must be involved as well.

On a different tack, the case for the less radiogenic melt inclusions sampling the depleted oceanic crust and lithosphere by assimilation is limited severely by the observation that, within analytical uncertainty, not a single melt inclusion has an $^{87}Sr/^{86}Sr$ ratio that is lower than the least radiogenic ($^{87}Sr/^{86}Sr=0.7044$) whole-rock basalt measured in the Samoan islands (Fig. 1). The Samoan melt inclusions trace out a range of Sr-isotope variability that is confined to the region of Sr-isotope space defined by the Samoan whole-rock data (Fig. 3). On an island-by-island basis, the interpretation is more complicated, as melt inclusions from two Vailulu'u whole-rocks sample a component more depleted than found in whole rocks measured from the seamount. However, the least radiogenic component found in Vailulu'u melt inclusions is also found in lavas from nearby Samoan islands (e.g., Ta'u and Ofu), exhibits elevated $^{3}He/^{4}He$ ratios, and is thus known to exist in the Samoan plume. Many of the downstream Samoan seamounts also are dominated by $^{87}Sr/^{86}Sr$ between 0.7044 and 0.7049 [3]. It seems unnecessary, therefore, to invoke contamination from the oceanic crust and lithosphere to explain the presence of the less radiogenic component when it already exists inside the plume! Although the argument can be made that an insufficient number of melt inclusions have been analyzed to detect a component more depleted than what is found in whole rocks, the number of melt inclusions analyzed for Sr isotopes ($n=41$) is already significant, and is equal to ~30% of the number of published $^{87}Sr/^{86}Sr$ whole-rock analyses from the Samoan hotspot.

The high $^{3}He/^{4}He$, unradiogenic Sr component in Samoan basalts (PHEM) is unique in that it exhibits $^{87}Sr/^{86}Sr$ ratios more enriched than in the high $^{3}He/^{4}He$ Hawaii, Iceland or Baffin Island basalts, suggesting that the high $^{3}He/^{4}He$ reservoir in the mantle is at least mildly heterogeneous in $^{87}Sr/^{86}Sr$ ratios. The same line of reasoning that precludes the presence of entrained melts from oceanic lithosphere in the Samoan melt inclusions also minimizes the possibility that a traditional, depleted FOZO-like component ($^{87}Sr/^{86}Sr=0.7030$ [24]) serves as the unradiogenic Sr component: If melt inclusion diversity were a result of entrainment of a component (MORB or FOZO) more depleted than found in Samoan basalts, then the melt inclusions would extend to $^{87}Sr/^{86}Sr$ ratios lower than found in whole rocks (0.7044). However, the high $^{3}He/^{4}He$ Samoan sample OFU-04-06 defines the lowest $^{87}Sr/^{86}Sr$ portion of the Samoan whole-rock mixing array (see Fig. 3) and the melt inclusions are identical to the whole rock, suggesting that the least radiogenic Sr composition sampled by the Ofu basalts is the same component found in the melt inclusions. Therefore, we maintain that the unradiogenic Sr component in Samoan melt inclusions is more enriched than MORB or FOZO, and is likely the same PHEM component sampled by the high $^{3}He/^{4}He$ Samoan basalts, suggesting that a two-component EM2–PHEM mixing model may be the most appropriate for melt inclusions originating in the enriched Samoan mantle. Scatter around such a mixing model (Fig. 8) may be due to minor contributions from other components [4] that may exist in the Samoan mantle.

4.4. Implications for source heterogeneity (or lack thereof)

The results for Sr-isotope measurements in Samoan melt inclusions support an argument for an origin of the isotopic variability in the melt source, not contamination by oceanic crust and lithosphere. We assume that the isotopic variability (or lack thereof) in Samoan melt inclusions is not a product of variable degrees of homogenization in magma conduits and chambers before olivine entrapment, but rather that the isotopic variability in melt inclusions reflects the heterogeneity of the melt source: When the melt source is heterogeneous, melt inclusions capture the range of heterogeneity while the isotopic composition of the bulk rock lava represents an average of the heterogeneity sampled in the melt. By extension, we infer that the high $^{3}He/^{4}He$ whole-rock sample OFU-04-06 tends to sample a more homogeneous source, as the melt inclusions are nearly isotopically homogeneous and identical to the bulk rock. Perhaps, then, only melting of a pure PHEM source allows the high $^{3}He/^{4}He$ composition to persist in the

Ofu whole-rock lavas. Vailulu'u and Malumalu melt inclusions are more isotopically heterogeneous, and thus are inferred to sample a heterogeneous source that captures much of the mixing spectrum between the EM2 and PHEM components. The contribution of an EM2 component may explain the diminished $^{3}He/^{4}He$ composition in the lavas from these two volcanoes. Although $^{87}Sr/^{86}Sr$ analyses of the melt inclusions from high $^{3}He/^{4}He$ basalts from other localities are not yet available, perhaps the high $^{3}He/^{4}He$ mantle that these basalts sample is homogeneous and devoid of enriched domains. This hypothesis is consistent with the melting–mixing model above (see Fig. 8), which suggests that the isotopically homogeneous melt inclusions from the high $^{3}He/^{4}He$ basalt from Ofu exhibit no evidence of mixing with an EM2 component.

It is notable that while near-pure PHEM melts are observed in Samoan melt inclusions, pure EM2 melts ($^{87}Sr/^{86}Sr=0.7128$ [4,36]) were not unequivocally detected in this study (i.e., by measurement of Sr isotopes). Several melt inclusions with ultra-enriched trace element patterns were observed, but most of the melt inclusions are composed of <30% EM2 component. Perhaps this indicates that, compared to the PHEM component, the EM2 component in the Samoan plume is rare. Alternatively, the EM2 component may not be rare in the Samoan plume, but is more refractory and produces less melt than the PHEM component. In this way, perhaps, EM2 melts are less frequently sampled by melt inclusions. Future work on melt inclusions will help resolve the relative contributions of the enriched and high $^{3}He/^{4}He$ sources to OIB lavas.

5. Summary

The following conclusions can be drawn from this study:

1.) The Sr-isotopic diversity in melt inclusions from Samoan basalts does not extend significantly above or below the range defined by whole rocks from the Samoan hotspot.
2.) A few melt inclusions exhibit $^{87}Sr/^{86}Sr$ ratios significantly higher than their host whole rock. This is taken as evidence that assimilation of MORB lithosphere cannot be the only mechanism that contributes isotopic diversity to the melt inclusions.
3.) The $^{87}Sr/^{86}Sr$ ratio of the high $^{3}He/^{4}He$ basalt is essentially indistinguishable from the Sr-isotope ratios (0.7044) measured in its melt inclusions, and the $^{87}Sr/^{86}Sr$ ratios in melt inclusions from other Samoan basalts do not exhibit ratios lower than 0.7044. This observation is consistent with the hypothesis that a high $^{3}He/^{4}He$ component, not MORB, is the unradiogenic Sr endmember in Samoan melt inclusions.
4.) Melt inclusions from a high $^{3}He/^{4}He$ Samoan basalt (with less radiogenic $^{87}Sr/^{86}Sr$) are isotopically more homogeneous than the melt inclusions from basalts with higher $^{87}Sr/^{86}Sr$ (more contribution from an EM2 component). This may indicate that the Samoan high $^{3}He/^{4}He$ basalts sample a source that is more isotopically homogeneous than the source that produces basalts with an EM2 component.

Acknowledgements

We thank Lary Ball for his generous analytical wizardry with the NEPTUNE. J. Blusztajn and R. Workman helped document the Sr-isotope basalt glass standards. We also thank N. Shimizu, A. Saal, M. Kurz, J. Wang, A. Koleszar and C. Waters for discussions. Simon Thorrold loaned us his sclerosponge standards, and helped with many technical discussions arising from his unparallel laser ablation Sr isotope work on carbonates. Frank Ramos provided a preprint of his paper, and numerous insightful discussions. Reviews from Vincent Salters and an anonymous reviewer greatly improved the manuscript. An NSF Graduate Research Fellowship is gratefully acknowledged (to MGJ). This research was supported by NSF grant EAR-0125917 (to SRH).

Appendix A. Supplementary data

Supplementary data associated with this article can be found, in the online version, at doi:10.1016/j.epsl.2006.02.040.

References

[1] A. Zindler, S.R. Hart, Chemical geodynamics, Annu. Rev. Earth Planet. Sci. 14 (1986) 493–571.
[2] A.W. Hofmann, Mantle geochemistry: the message from oceanic volcanism, Nature 385 (1997) 219–229.
[3] S.R. Hart, M. Coetzee, R.K. Workman, J. Blusztajn, K.T.M. Johnson, J.M. Sinton, B. Steinberger, J.W. Hawkins, Genesis of the Western Samoa seamount province: age, geochemical fingerprint and tectonics, Earth Planet. Sci. Lett. 227 (2004) 37–56.
[4] R.K. Workman, S.R. Hart, M. Jackson, M. Regelous, K.A. Farley, J. Blusztajn, M. Kurz, H. Staudigel, Recycled metasomatized lithosphere as the origin of the Enriched Mantle II (EM2) endmember: evidence from the Samoan volcanic chain, Geochem. Geophys. Geosyst. 5 (2004), doi:10.1029/2003GC000623.

[5] W.J. Morgan, Convection plumes in the lower mantle, Nature 230 (1971) 42–43.
[6] R.K. Workman, E. Hauri, S.R. Hart, J. Wang, J. Blusztajn, Volatile and trace elements in basaltic glasses from Samoa: implications for water distribution in the mantle, Earth Planet. Sci. Lett. 24 (2006) 932–951.
[7] L.V. Danyushevsky, M.R. Perfit, S.M. Eggins, T.J. Falloon, Crustal origin for coupled 'ultra-depleted' and 'plagioclase' signatures in MORB olivine-hosted melt inclusions: evidence from the Siquieros Transform Fault, East Pacific Rise, Contrib. Mineral. Petrol 144 (2003) 619–637.
[8] L.V. Danyushevsky, R.A.J. Leslie, A.J. Crawford, P. Durance, Melt inclusions in primitive olivine phenocrysts: the role of localized reaction processes in the origin of anomalous compositions, J. Pet. 45 (2004) 2531–2553.
[9] A.V. Sobolev, N. Shimizu, Ultra-depleted primary melt included in an olivine from the Mid-Atlantic Ridge, Nature 363 (1993) 151–154.
[10] A.A. Gurenko, M. Chaussidon, Enriched and depleted primitive melts included in olivine from Icelandic tholeiites: origin by continuous melting of a single mantle column, Geochim. Cosmochim. Acta 59 (1995) 2905–2917.
[11] J.C. Lassiter, E.H. Hauri, I.K. Nikogosian, H.G. Barsczus, Chlorine–potassium variations in melt inclusions from Raivavae and Rapa, Austral Islands: constraints on chlorine recycling in the mantle and evidence for brine-induced melting of oceanic crust, Earth Planet. Sci. Lett. 202 (2002) 525–540.
[12] E. Cottrell, M. Spiegelman, C.H. Langmuir, Consequences of diffusive reequilibration for the interpretation of melt inclusions, Geochem. Geophys. Geosyst. 3 (2002), doi:10.1029/2001GC000205.
[13] G.A. Gaetani, E.B. Watson, Modeling the major-element evolution of olivine-hosted melt inclusions, Chem. Geol. 183 (2002) 25–41.
[14] G.A. Gaetani, E.B. Watson, Open system behavior of olivine-hosted melt inclusions, Earth Planet. Sci. Lett. 183 (2000) 27–41.
[15] P. Schiano, R. Clocchiatti, Worldwide occurrence of silica-rich melts in sub-continental and sub-oceanic mantle minerals, Nature 368 (1994) 621–624.
[16] V. Kamenetsky, Methodology for the study of melt inclusions in Cr-spinel, and implications for parental melts of MORB from FAMOUS area, Earth Planet. Sci. Lett. 142 (1996) 477–484.
[17] A.E. Saal, S.R. Hart, N. Shimizu, E.H. Hauri, G.D. Layne, Pb isotopic variability in melt inclusions from oceanic island basalts, Polynesia, Science 282 (1998) 1481–1484.
[18] K. Kobayashi, R. Tanaka, T. Moriguti, K. Shimizu, E. Nakamura, Lithium, boron, and lead isotope systematics of glass inclusions in olivines from Hawaiian lavas: evidence for recycled components in the Hawaiian plume, Chem. Geol. 212 (2004) 143–161.
[19] H. Yurimoto, T. Kogiso, K. Abea, H.G. Barsczus, A. Utsunomiya, S. Maruyama, Lead isotopic compositions in olivine-hosted melt inclusions from HIMU basalts and possible link to sulfide components, Phys. Earth Planet. Inter. 146 (2004) 231–242.
[20] K.P. Jochum, B. Stoll, A.W. Hofmann, Pb isotopes and trace elements in melt inclusions from Hawaiian basalts using LA-ICPMS and SRXRF, Geochim. Cosmochim. Acta 68 (Sup.1) (2004) A564.
[21] A.E. Saal, S.R. Hart, N. Shimizu, E.H. Hauri, G.D. Layne, J.M. Eiler, Pb isotopic variability in melt inclusions from the EMI–EMII–HIMU mantle end-members and the role of the oceanic lithosphere, Earth Planet. Sci. Lett. 240 (2005) 605–620.
[22] Y. Su, C.H. Langmuir, Global MORB chemistry compilation at the segment scale, Ph.D. Thesis, Department of Earth and Environmental Sciences, Columbia University (2003). Available at: http://petdb.ldeo.columbia.edu/documentation/morbcompilation/.
[23] K.A. Farley, J.H. Natland, H. Craig, Binary mixing of enriched and undegassed (primitive?) components (He, Sr, Nd, Pb) in Samoan lavas, Earth Planet. Sci. Lett. 111 (1992) 183–199.
[24] S.R. Hart, E.H. Hauri, L.A. Oschmann, J.A. Whitehead, Mantle plumes and entrainment—isotopic evidence, Science 256 (1992) 517–520.
[25] M.G. Jackson, M.D. Kurz, S.R. Hart, R. Workman, Implications of new high $^{3}He/^{4}He$ values from the Samoan hotspot, Abstr. EOS Tran. AGU, 86, Fall Meet. Suppl., 2005, pp. V41D–V1485.
[26] F.C. Ramos, J.A. Wolff, D.L. Tollstrup, Measuring $^{87}Sr/^{86}Sr$ variations in minerals and groundmass from basalts using LA-MC-ICPMS, Chem. Geol. 211 (2004) 135–158.
[27] N. Shimizu, C.J. Allegre, Geochemistry of transition elements in garnet lherzolite nodules in kimberlites, Contrib. Mineral. Petrol. 67 (1978) 41–50.
[28] N. Shimizu, A.P. Le Roex, The chemical zoning of augite phenocrysts in alkaline basalts from Gough Island, South Atlantic, J. Volcanol. Geotherm. Res. 29 (1978) 149–199.
[29] P.L. Roeder, R.F. Emslie, Olivine-liquid equilibrium, Contrib. Mineral. Petrol. 29 (1970) 275–289.
[30] W.F. McDonough, S.S. Sun, The composition of the Earth, Chem. Geol. 120 (1995) 223–253.
[31] N. Shimizu, The geochemistry of olivine-hosted melt inclusions in a FAMOUS basalt ALV519-4-1, Phys. Earth Planet. Inter. 107 (1998) 183–201.
[32] H.J.B. Dick, R.L. Fisher, W.B. Bryan, Mineralogic variability of the uppermost mantle along the mid-ocean ridges, Earth Planet. Sci. Lett. 69 (1984) 88–106.
[33] P.B. Kelemen, G.M. Yogodzinski, D.W. Scholl, Along-strike variation in lavas of the Aleutian island arc: implications for the genesis of high Mg# andesite and the continental crust, in: J. Eiler (Ed.), Inside the Subduction Factory, AGU Monograph, vol. 138, AGU, 2004, pp. 223–276.
[34] E. Takazawa, F. Frey, N. Shimizu, M. Obata, Evolution of the Horoman peridotite (Hokkaido, Japan): implications from pyroxenite compositions, Chem. Geol. 134 (1996) 3–26.
[35] R.K. Workman, S.R. Hart, Major and trace element composition of the depleted MORB mantle (DMM), Earth Planet. Sci. Lett. 231 (2005) 53–72.
[36] E.H. Hauri, N. Shimizu, J. Dieu, S.R. Hart, Evidence for hotspot-related carbonatite metasomatism in the oceanic upper mantle, Nature 365 (1993) 221–227.
[37] M.D. Kurz, W.J. Jenkins, S.R. Hart, D. Clague, Helium isotopic variations in volcanic rocks from Loihi seamount and the Islands of Hawaii, Earth Planet. Sci. Lett. 66 (1983) 388–406.
[38] D.R. Hilton, K. Grönvold, C.G. Macpherson, P.R. Castillo, Extreme $^{3}He/^{4}He$ ratios in northwest Iceland: constraining the common component in mantle plumes, Earth Planet. Sci. Lett. 173 (1999) 53–60.
[39] F.M. Stuart, S. Lass-Evans, J.G. Fitton, R.M. Ellam, High $^{3}He/^{4}He$ ratios in picritic basalts from Baffin Island and the role of a mixed reservoir in mantle plumes, Nature 424 (2003) 57–59.
[40] P.J. Valbracht, T. Staudacher, A. Malahoff, C.J. Allegre, Noble gas systematics of deep rift zone glasses from Loihi Seamount, Hawaii, Earth Planet. Sci. Lett. 150 (1997) 399–411.
[41] S. Lass-Evans, The anatomy of the ancestral Iceland plume: a chemical and isotopic study of the Tertiary basalts and picrites from Baffin Island, Ph.D. Thesis, School of GeoSciences, University of Edinburgh (2005).